RSC Advances

ROYAL SOCIETY OF CHEMISTRY

www.rsc.org/advances

Journal Name

ARTICLE

Fluorescent properties of dissolved organic matter as functions of hydrophobicity and molecular weight? Case studies from two membrane bioreactors and an oxidation ditch

Received 00th January 20xx,
Accepted 00th January 20xx

DOI: 10.1039/x0xx00000x

www.rsc.org/

Kang Xiao,[a,b] Jian-yu Sun,[b] Yue-xiao Shen,[b] Shuai Liang,[b] Peng Liang,[b] Xiao-mao Wang*[b] and Xia Huang*[b]

Dissolved organic matter (DOM) plays substantial roles in wastewater treatment systems. Fluorescence is an important nature of DOM and is promising for DOM characterization, but has rarely been extended to probing the basic physicochemical properties such as hydrophobicity and molecular weight. This study explores the possible linkages between fluorescent properties and hydrophobicity/molecular weight of DOM, through case studies from three wastewater treatment plants (two membrane bioreactors and one oxidation ditch). The fluorescent properties of different hydrophobic/hydrophilic and molecular-weight fractions of DOM were obtained using excitation-emission matrix (EEM) spectroscopy and size-exclusion chromatography with fluorescence detection. The EEM spectra were intepreted using techniques of fluorescence regional integration, parallel factor analysis, fluorescence spectroscopic indices, and a novel energetic mapping based on fluorophore energy levels. It was found that in all the three plants, the hydrophobic fractions of DOM had higher fluorescence intensity per UV absorbance (indicating higher quantum yield) as well as larger Stokes shifts than the hydrophilic fraction. The lower-molecular-weight fractions generally exhibited higher fluorescence intensity per total organic carbon (indicating higher fluorophore density), with the fluorescence distributed at slightly smaller excitation and emission wavelengths. These phenomena were explained via analysis of fluorophore energy state during the excitation/emission process. The scale of π-conjugated system in DOM molecules may serve as an intermediate factor for the correlations between hydrophobicity/molecular weight and these fluorescent properties. These correlations may assist in developing fluorescent proxies for DOM characteristics during process monitoring of wastewater treatment plants.

Introduction

Dissolved organic matter (DOM) plays an important role in wastewater treatment systems. DOM in the mixed liquor is inextricably linked to various processes during wastewater treatment.[1,2] It can have fundamental impacts on many physicochemical processes, such as sludge sedimentation, coagulation, adsorption, and membrane filtration.[3-5] Among the physicochemical properties of DOM, hydrophobicity and molecular size/weight are important representatives.[1] Hydrophobicity has a significant impact on the interfacial interactions between DOM and surfaces/particles/colloids/solutes, and can affect basic behaviors of separation, such as phase partitioning, interfacial adsorption, colloidal stability, and biopolymer solubility.[6] Molecular size/weight is closely related to the steric behavior of DOM, such as diffusive mass transfer and mechanical interception (sieving effect).[7] For conventional activated sludge processes like oxidation ditch (OD), hydrophobicity of DOM can affect the partition between soluble and bound extracellular polymers, which are well-reported influencers of sludge settleability;[8] while molecular weight of DOM may impact on the mixed liquor viscosity.[9] In membrane filtration processes like membrane bioreactor (MBR), DOM acts as a major cause of membrane fouling which is a critical concern for filtration efficiency.[4] The hydrophobicity of DOM governs its mass balance among sludge, water, and the membrane surface,[10,11] while the molecular size influences the membrane sieving effect and hence membrane pore blockage.[7] Both the hydrophobicity and molecular size have been regarded as principal factors in membrane fouling.[7,12]

These properties of DOM may thus serve as indicators of treatment performance (e.g. sludge settleability and membrane retention efficiency) and operational state (e.g. sludge activity, difficulty of separation, and propensity for membrane fouling) of the processes. Real-time continuous monitoring of the DOM characteristics, if achievable, will provide a quick grasp of the state of wastewater treatment, and will help to optimize the process operation. For example, dynamic feedback of the DOM property data will be useful for working out preventive measures to tackle membrane fouling, by timely

[a] College of Resources and Environment, University of Chinese Academy of Sciences, Beijing 100049, China.
[b] State Key Joint Laboratory of Environment Simulation and Pollution Control, School of Environment, Tsinghua University, Beijing 100084, China. E-mail: wangxiaomao@tsinghua.edu.cn (X. Wang); xhuang@tsinghua.edu.cn (X. Huang); Tel: 86-10-62781386 (X. Wang); +86-10-62772324 (X. Huang)
Electronic Supplementary Information (ESI) available. See DOI: 10.1039/x0xx00000x

adjustments of filtration conditions. Therefore, real-time DOM monitoring is expected to form a potentially critical part of the automated control and refined management of future wastewater treatment plants (WWTPs).

Despite their usefulness for monitoring wastewater treatment processes, DOM hydrophobicity and molecular size/weight are not convenient to measure. Conventional methods (such as adsorptive column chromatographic fractionation for hydrophobicity assessment,[13] and size-exclusion chromatography for molecular weight profiling[14]) are usually complicated and time-consuming, therefore difficult to achieve rapid online monitoring. To be contrary in this regard, excitation-emission matrix (EEM) fluorescence spectroscopy is an attractive method, rapid and sensitive for DOM characterization.[15-17] Following light absorption, the excited fluorophores of DOM undergo relaxation and emit fluorescence.[18] A continuous scan of fluorescence signal across a certain range of excitation wavelength (Ex) and emission wavelength (Em) yields a three-dimensional EEM spectrum, in which fluorescence intensity is plotted as a function of Ex and Em. Due to its sensitive dependence upon fluorephore properties, EEM fluorescence spectroscopy has been remarked as a useful tool to "fingerprint" DOM characteristics.[17,19,20]

The question is whether EEM fluorescence can be used to probe the properties (hydrophobicity and molecular weight) of DOM in wastewater treatment systems. Different properties of fluorophore in chemical structure, molecular polarity (related to hydrophobicity) and molecular size/weight will lead to differences in EEM signals.[21,22] Therefore, it must be theoretically feasible to use EEM in turn to indicate differences in hydrophobicity and molecular weight of DOM. It is speculated that for DOM in a certain unit of a wastewater treatment process, if there is any measurable change in the hydrophobicity or molecular weight change, its fluorescence will change accordingly in a predictable way. To achieve fast monitoring of hydrophobicity and molecular weight based on the fluorescent method, it is critical to establish the possible relations between fluorescence spectral information and these DOM properties.

Since DOM is a heterogeneous mixture of organics, a preliminary approach to examining these relations, in principle, is to split DOM into components with different hydrophobicity and molecular sizes, and to find out if there is any definite difference in their fluorescence. Typical components in this regard include hydrophobic acids/bases/neutrals (HOA/HOB/HON) and hydrophilic substances (HIS);[1] each could be subdivided according to molecular weight from < 1 kDa to > 100 kDa.[23] It is conceivable that the overall fluorescence of DOM is most likely to be intermediate among that of the components, and vary within the limits of the components. The distinction in fluorescence among these components is considered to be a fundamental condition for the relationship between the overall fluorescence and hydrophobicity/molecular weight of DOM. A few researchers have noted some variations of fluorescence with DOM components according to hydrophobicity and molecular weight,[5,14] while the detailed and definite relationship is yet to be systematically unveiled.

This study aims to explore the relationship between EEM fluorescent properties and hydrophobicity/molecular weight of DOM in wastewater treatment systems. Two MBRs and an OD plant were selected for the case studies, allowing cross-examination of the influences of wastewater origin and process configuration. DOM was fractionated into different hydrophobic/hydrophilic and molecular-weight components. The information embedded in the EEM spectrum of each fraction was thoroughly explored. Combined utilization of the techniques of fluorescence regional integration (FRI)[21], parallel factor analysis (PARAFAC)[24], fluorescence spectroscopic indices based on ratios of fluorescence intensity which indicate the origin of DOM,[25] and high performance size-exclusion chromatography–fluorescence detection (HPSEC-FLD)[14] enabled analyses from multiple aspects. More importantly, inner information of fluorescence, such as fluorophore density, quantum yield,[26,27] and fluorophore energetic properties (e.g. Stokes shift and energy state),[18,22] were further extracted from EEM. On this basis, we tried to find out if there would be any definite difference between the DOM fractions to infer reasonable linkage between these fluorescence parameters and hydrophobicity/molecular weight of DOM.

Materials and methods

Overview of the case studies

The DOM for this study was obtained from the mixed liquor of three full-scale WWTPs: "B" and "C" membrane bioreactors (BM and CM), and "C" oxidation ditch (CO) in China. BM was fed with domestic wastewater, while CM and CO were operated in parallel sharing the same municipal wastewater with an industrial portion of around 40%. All the three plants had large treatment capacities (60,000 m^3/d for BM and 50,000 m^3/d for CM and CO), and guaranteed simultaneous removal of nitrogen and phosphorous, with the detailed process flows shown in the Supplementary Information (Fig. S1). Both BM and CM comprised anaerobic, anoxic, aerobic, and membrane tanks in sequence, while CO included an Orbal-type oxidation ditch followed by a sedimentation tank. All of the three plants were in stable operation during the period of DOM sampling.

DOM sampling

The sludge mixed liquor was sampled from the aerobic zones of the three WWTPs (i.e., the aerobic tanks of BM and CM, and the inner channel of the Orbal oxidation ditch of CO). Considering the aerobic zone had the longest hydraulic retention time in the process of each WWTP, samples from this zone should be the best representative of the mixed liquor of the overall process. DOM was then extracted from the mixed liquor in the sequence of: centrifugation (CF16RX II, Hitachi, Japan) at 3,000×*g* and 4°C for 5 min, coarse filtration of the supernatant with filter paper, and fine filtration with 0.7 μm glass-fiber membrane (GF/F, Whatman, UK). The resultant filtrate was regarded as the DOM solution.

DOM fractionation based on hydrophobicity and molecular weight

DOM was fractionated into HOA, HOB, HON, and HIS, according to the well-applied adsorptive column chromatographic procedure[1,12] using the nonionic Supelite DAX-8 resin (Supelco, USA). Briefly speaking, HOA is adsorbed by the resin at lower pH but released at higher pH, while HOB behaves inversely; HON is adsorbed at any pH, while HIS is not adsorbable over the whole pH range. HOA, HOB, and HON were eluted from the resin by 0.1 M NaOH, 0.1M HCl, and methanol, respectively. All these hydrophobic/hydrophilic fractions obtained were then diluted back to the same volume as the original DOM solution, with pH adjusted to neutral.

The hydrophobic/hydrophilic fractions of DOM were further subdivided into different molecular-size/weight grades via successive ultrafiltration,[28] using a series of regenerated cellulose membranes with nominal molecular-weight cutoffs of 100 kDa, 10 kDa, and 1kDa (PLHK, PLGC, and PLAC, Millipore, USA). The molecular-size/weight grades of the DOM fractions before and after the series of ultrafiltration were thus <0.7 μm, <100 kDa, <10 kDa, and <1 kDa, respectively. The ultrafiltration was performed in a stirred dead-end filtration cell (Amicon 8400, Millipore, USA) at constant pressure, with the stirring rate set at 170 rpm to mitigate concentration polarization.

Total organic carbon (TOC) and concentrations of polysaccharides, proteins, and humics were employed to characterize the distribution of DOM mass among different hydrophobic/hydrophilic and molecular-weight fractions. TOC was determined using a TOC analyzer (TOC-VCPH, Shimadzu, Japan). Polysaccharides were quantified according to the phenol-sulfuric acid assay.[29] Proteins and humics were detected using the modified Lowry method, with the interfering hardness ions removed prior to the measurement.[30]

EEM fluorescence spectroscopy

Three-dimensional EEM spectra of the DOM fractions were measured using a fluorescence spectrophotometer (F-7000, Hitachi, Japan). The fluorescence was scanned in the 3-D mode over the wavelength ranges of Ex = 200–400 nm for excitation and Em = 250–500 nm for emission, with a scan speed of 2400 nm/min and an interval of 5 nm. The slit widths for excitation and emission were both 5 nm, and the voltage of the photomultiplier detector was set at 700 V. Prior to the measurement, the pH of each sample was adjusted to 7.0. The EEM spectrum for each sample were measured twice and averaged. The EEM properties of HON were not studied here, considering that methanol contained in HON might change the polarity of the solvent and interfere in the fluorescence measurement.[31]

The original EEM spectra were then corrected and standardized, following the procedure illustrated in Fig. S2. Firstly, background signals (i.e. pure water spectra) were subtracted from the EEM spectra; secondly, the interfering signals of the first- and second-order Rayleigh and Raman scattering were removed using an interpolation technique;[32] thirdly, the fluorescence intensity was corrected for the inner-filter effect using the UV-visible absorption spectra (UV-2401PC, Shimadzu, Japan) in the range of 200–500 nm;[18,33] finally, the fluorescence intensity was calibrated into Raman Units (R.U.) to remove instrument-dependent factors,[34] and was divided by TOC concentration to obtain the specific fluorescence intensity (S.F.I.).

The standardized EEM spectra were analyzed to harvest fluorecence information. Ordinary information includes: (a) location and intensity of fluorescence peaks, which were directly read from the 3-D spectrum; (b) independent fluorecent components, which were identified following the PARAFAC protocol;[24] (c) distribution of fluorecence over different EEM regions, characterized using the FRI method;[21] and (d) fluorescence indices based on intensity ratios, including the f_{450}/f_{500} index, the humification index (HIX), and the biological index of recent autochthonous contribution (BIX), which may provide clues about the origin of DOM.[25] The PARAFAC calculation was performed using the MATLAB R2012b software, with 13 fluorescence samples (DOM fractions) included for each WWTP. In the FRI method, an EEM map is typically divided into five regions (denoted as I–V), which are assigned to protein-like (I and II), fulvic acid-like (III), soluble microbial byproduct-like (IV), and humic acid-like (V) substances. The fluorescence intensity in each region was integrated to calculate the percentage regional contribution to the total fluorescence. The f_{450}/f_{500} index was the ratio of fluorescence intensity at Em 450 nm to that at Em 500 nm, given Ex = 370 nm. HIX was obtained via dividing the integrated intensity of Em = 435–480 nm by that of Em = 300–345 nm at Ex 254 nm. BIX was the ratio of fluorescence intensity at Em 380 nm to that at Em 430 nm, given Ex = 310 nm. Larger f_{450}/f_{500} and BIX, and smaller HIX values, may indicate a higher probability that the DOM has been freshly produced from biological activity.[25] In-depth fluorecence information was further extracted from the EEM spectra, including: (a) overall quantum yield, which was derived by comparing the total fluorescence intensity with the total UV absorbance;[26,27] (b) Stokes shift, calculated from the difference between excitation and emission light frequencies;[18,22] and (c) overall energy level of the excited state, which can be reflected by Ex and Em;[18,22] and was estimated here as negatively related to the root-mean-square (RMS) of Ex and Em.

HPSEC-FLD

HPSEC-FLD was utilized to further inspect the dependence of fluorescence on molecular weight distribution for each hydrophobic/hydrophilic fraction. A fluorescence detector (FLD) was incorporated into the gel permeation/size-exclusion chromatography system (HPLC 1200 Series, Agilent Technologies, USA). The gel column (PL aquagel-OH MIXED 8 μm, Agilent Technologies, USA) allows for the separation of the solutes from 0.1 to 600 kDa. For each sample, a volume of 100 μL was injected, and was eluted with 4 g/L NaCl aqueous solution at a flow rate of 0.3 mL/min at 30 °C. Prior to injection, the conductivity of each sample was adjusted to that of the eluent. The fluorescence signals of the effluent were recorded continuously at the Ex/Em wavelengths (nm) of 230/340, 250/430, 280/340, and 310/390, corresponding to the typical fluorescence regions for proteins, fulvic acids, microbial byproducts, and humic acids,

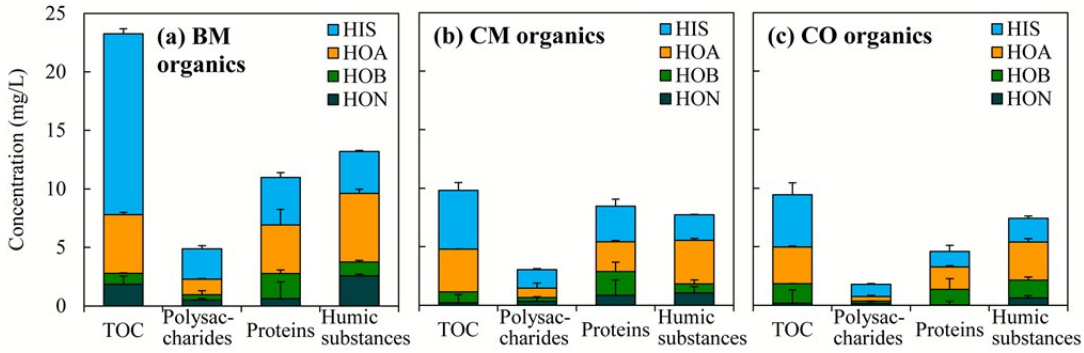

Fig. 1 Distribution of hydrophobic/hydrophilic fractions of DOM from the three wastewater treatment plants, denoted as (a) BM, (b) CM, and (c) CO plants. HIS = hydrohilic substances, HOA = hydrophobic acids, HOB = hydrophobic bases, HON = hydrophobic neutrals.

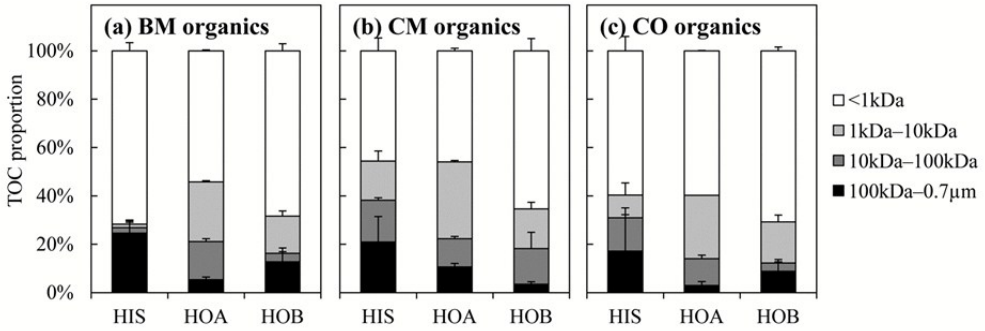

Fig. 2 Molecular weight distribution of DOM fractions from the BM, CM, and CO plants.

respectively.[21] In addition, refractive index (RI) of the effluent was also monitored to reflect the overall amount of organic matter as a complement to the fluorescence signals.

Results and discussion

Hydrophobicity and molecular weight distributions of DOM

The hydrophobicity and molecular weight distributions of the DOM from the three WWTPs are shown in Fig. 1 and Fig. 2, respectively. Both the hydrophobic portion (as a sum of HOA, HOB, and HON) and the hydrophilic portion (HIS) had significant shares in the TOC concentration for all the three WWTPs (Fig. 1). This suggests that the fluorescent properties of both portions are worth studying.

As to the chemical composition of the DOM (Fig. 1), polysaccharides mainly behaved as HIS, and humics were mainly enriched in HOA. Proteins took a larger proportion than polysaccharides and humics in HOB. The distribution of these chemical species in the hydrophobic/hydrophilic fractions agrees well with the nature of the typical functional groups of these species. Polysaccharides contain an abundant amount of hydroxyl groups in the sugar units,[35] giving rise to the generally more pronounced hydrophilicity than proteins and humics.[11] Aromatic amines in proteins and aromatic acids in humics are normally responsible for the hydrophobicity of HOB and HOA, respectively.[1]

The hydrophobicity distributions of DOM from the three WWTPs were not all the same (Fig. 1). The DOM from the BM plant had the highest proportion of HIS (accounting for 67% in TOC concentration). The contents of polysaccharides, proteins, and humics per unit TOC were generally low in the BM organics, which was particularly significant for humics (0.57 g/gTOC compared with 0.79 and 0.78 g/gTOC in CM and CO organics). These contents may indicate the functional group density. The functional groups refer to sugar units,[29] peptide bonds,[36] and phenolic hydroxyl groups,[37] respectively, according to the specific methods for measuring polysaccharides (the phenol-sulfuric acid assay[29]), and proteins and humics (the modified Lowry method[30]). The CM and CO organics were similar in hydrophobicity distribution, except that the CM organics had higher contents of HOB and proteins (cf. Fig. 1(b) and (c)).

The DOM from the three WWTPs all showed a broad molecular weight distribution (Fig. 2). For each of the HIS, HOA, and HOB fractions, the molecualr weight distributions were similar among the three WWTPs (except for HIS of BM). The low-molecular-weight substances (<1 kDa) formed the major portion in all of the fractions (especially in HOB). The high- and middle-molecular-weight substances (>100 kDa and 1–100 kDa) were prominent mainly in HIS and HOA, respectively. It is thus speculated that the average molecular weight of the hydrophobic/hydrophilic fractions might follow the order HIS > HOA > HOB. This is consistent with the general recognition that poly-

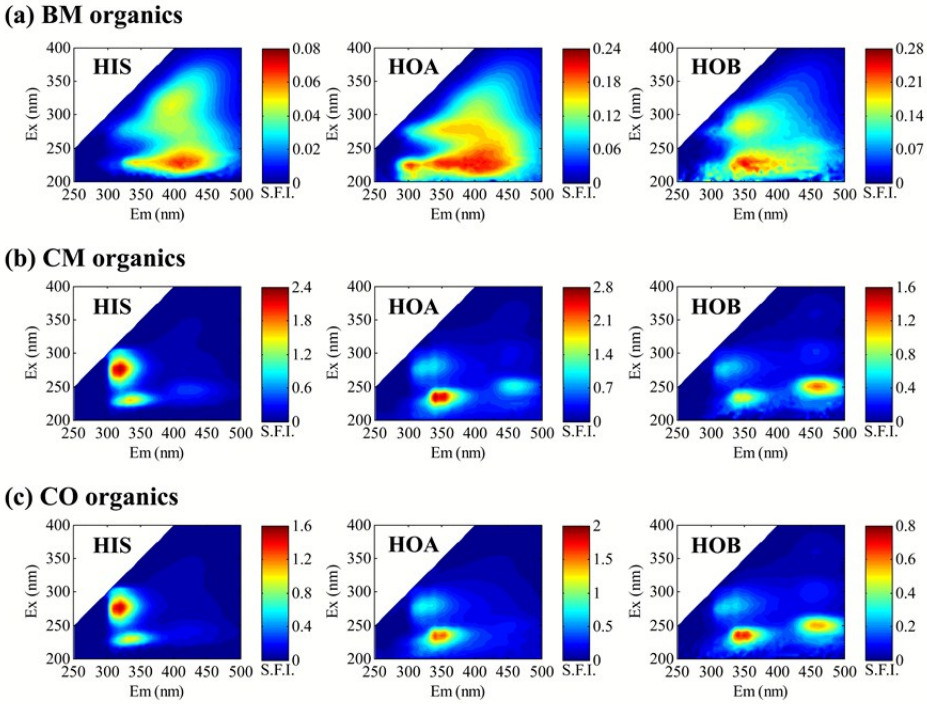

Fig. 3 Three-dimensional EEM fluorescence spectra of DOM fractions from the BM, CM, and CO plants.

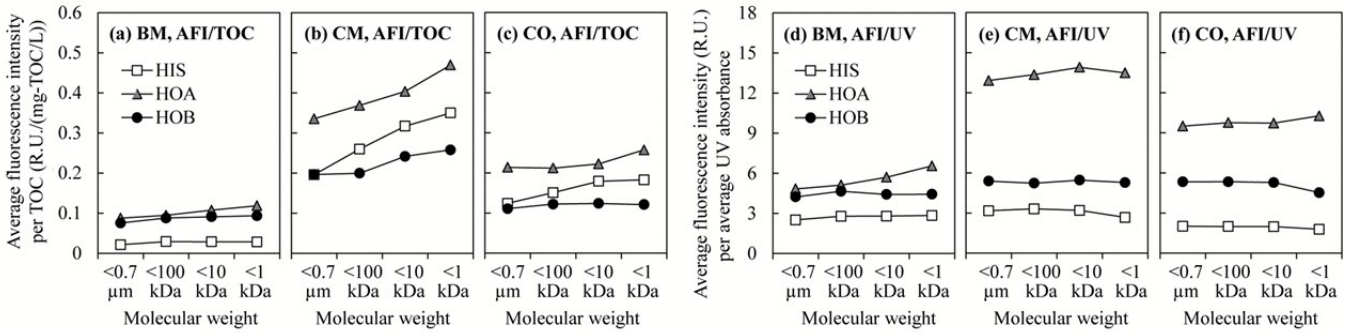

Fig. 4 Average fluorescence intensity per unit TOC (AFI/TOC, a–c) and average fluorescence intensity per average UV absorbance (AFI/UV, d–f) of DOM fractions from the BM, CM, and CO plants. The fluorescence intensity is averaged over the wavelengths of Ex = 200–400 nm and Em = 250–500 nm. The UV absorbance is averaged over the wavelengths of 200–400 nm.

saccharides usually have larger average molecular size than humics in the aqueous phase of WWTPs.[28,38,39]

The wide distributions of hydrophobicity and molecular weight, as shown above, would be favorable for comparison among different fractions, in order to reveal the possible influence of these properties on fluorescence.

EEM spectra of DOM fractions

The EEM spectra of the DOM from the three WWTPs are presented in Fig. 3. Different hydrophobic/hydrophilic fractions exhibit different EEM spectra. For each fraction, the spectrum of CM organics looks similar to that of CO organics, but both were quite unlike that of BM organics, which might be ascribed to the different wastewater sources of the three WWTPs. From the appearance of EEM spectra alone, however, it is difficult to make precise comparison among either the fractions or the WWTPs.

PARAFAC analysis was performed to extract the major fluorescent components from the EEM spectra, with the components plotted in Fig. S3. Peak locations of each component, as well as its contrbution rate to the overall fluorescence, are given in Table S1. The components basically covered the typical fluorescent substances of aromatic proteins, soluble microbial byproducts, humic acids, and fulvic acids. By comparison among the hydrophobic/hydrophilic fractions of DOM (Table S1), the fluorescence contribution rates of the PARAFAC components were different, with the hydrophobic fractions presented higher proportions of the “A” and “B” components but lower proportion of “D”. The difference might be somehow explained from the perspective of chemical composition. The

comparison among the three WWTPs, however, was complicated so that it is difficult to draw a general conclusion.

Detailed fluorescent properties of DOM fractions with varied hydrophobicity and molecular weight

Fluorescence intensity per TOC. Fig. 4(a–c) shows the average fluorescence intensity per unit TOC (AFI/TOC) of the DOM fractions from the three WWTPs. Here the fluorescence intensity (in R.U.) was averaged over the EEM region of Ex = 200–400 nm and Em = 250–500 nm (Ex < Em). AFI/TOC may grossly reflect the overall fluorophore density (notwithstanding the possible side effect of fluorescence quenching which attenuates AFI/TOC[18]). This quantity increased with decreasing molecular weight, as a general tendency for all the three WWTPs (Fig. 4(a–c)). Smaller molecules of DOM seemed to have higher fluorophore density in the present systems, which accords well with some previous reports.[40] This might be attributed to the larger specific surface area for exposure to light on the one hand, and the intrinsically higher fluorophore density for smaller molecules (if possible) on the other hand.

The average fluorescence intensity per unit TOC also varied with hydrophobicity. Among the hydrophobic/hydrophilic fractions, HOA showed the highest value for all the three WWTPs (Fig. 4(a–c)). For the BM plant which treated domestic wastewater, HIS exhibited the lowest AFI/TOC, likely due to the lower content of fluorescent species like proteins and humics. But for the CM and CO plants which were fed with a mixture of domestic and industrial wastewaters, the AFI/TOC levels of HIS were largely elevated, probably because HIS contained some highly fluorescent substances of industrial origin. The distinct EEM peaks of HIS for CM and CO plants (Fig. 3) may be a sign of the special fluorescent susbstances.

Fluorescence intensity per UV absorbance. Fig. 4(d–f) shows the ratio of average fluorescence intensity to average UV absorbance (AFI/UV) of the DOM fractions from the three WWTPs. Here the UV absorbance was averaged over the wavelengths of 200–400 nm. This ratio can partly evaluate the fluorescent quantum yield.[26,27] It can be inferred from Fig. 4(d–f) that the quantum yields of the hydrophobic/hydrophilic fractions followed the order HOA > HOB > HIS for all of the three WWTPs. The higher quantum yields of HOA and HOB could be related to the higher aromaticity. HOA had a high content of humic substances (Fig. 1). The large π-conjugated systems due to the polycyclic aromatic structure of humic substances[41] could largely enhance the quantum yield. HOB contained aromatic protein groups (e.g. tryptophan, tyrosine, and phenylalanine) with high quantum yield, but quenching of fluorescence (i.e. decrease of quantum yield) might occur among these groups to some extent. Particularly, $-NH_3^+$, –COOH, and other electron deficient groups could affect n–π* electronic transitions.[18,22] For HIS which had higher content of polysaccharides and lower aromaticity, the lack of large π-conjugated systems could be responsible for the low quantum yield. Yamaguchi et al.[42] showed quantitatively that for compounds with similar structure, a larger π-conjugated system (quantified by π-conjugation length) renders longer excited-state lifetime and thus greater fluorescent quantum yield.

FRI and fluorescence indices. Fig. S4 and Fig. S5 presents, respectively, the FRI results and the fluorescence indices (i.e. f_{450}/f_{500}, HIX, and BIX) for the DOM fractions with varied hydrophobicity and molecular weight. The values of $f_{450}/f_{500} > 1.5$, HIX < 4.4, and BIX > 0.9 for all the fractions suggested a strong biological contribution to the origin of these organics. The FRI distribution over the five typical EEM regions, as well as the fluorescence index values, differed among the hydrophobic/hydrophilic fractions. However, the three different WWTPs failed to guarantee a universal trend in the hydrophobicity-dependent FRI distribution and fluorescence indices.

Analysis of fluorophore energy state. The entire process of fluorescence typically consists of absorption of incident light, electronic excitation, vibrational relaxation, fluorescence emission, and non-radiative decay (in the form of e.g. heat dissipation) or quenching.[22] Scheme 1(a) displays a simplified diagram of the energy states of fluorophore in the process. The energy of emission is typically lower than that of excitation, due to vibrational relaxation. This energy loss is proportional to the frequency difference between the excitation and emission (i.e. Ex^{-1}–Em^{-1}, which is defined as Stokes shift[22]). Stokes shift can offer valuable molecular information on fluorophore structure and chemical environment.[18] In addition, from the excitation

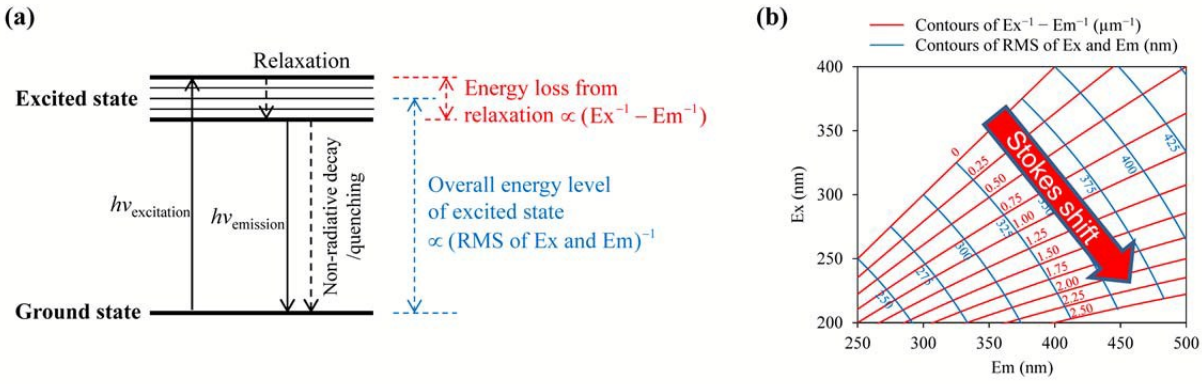

Scheme 1 Illustration of energy change during fluorescence process (a), and contours of fluorophore energy state on an EEM map (b).

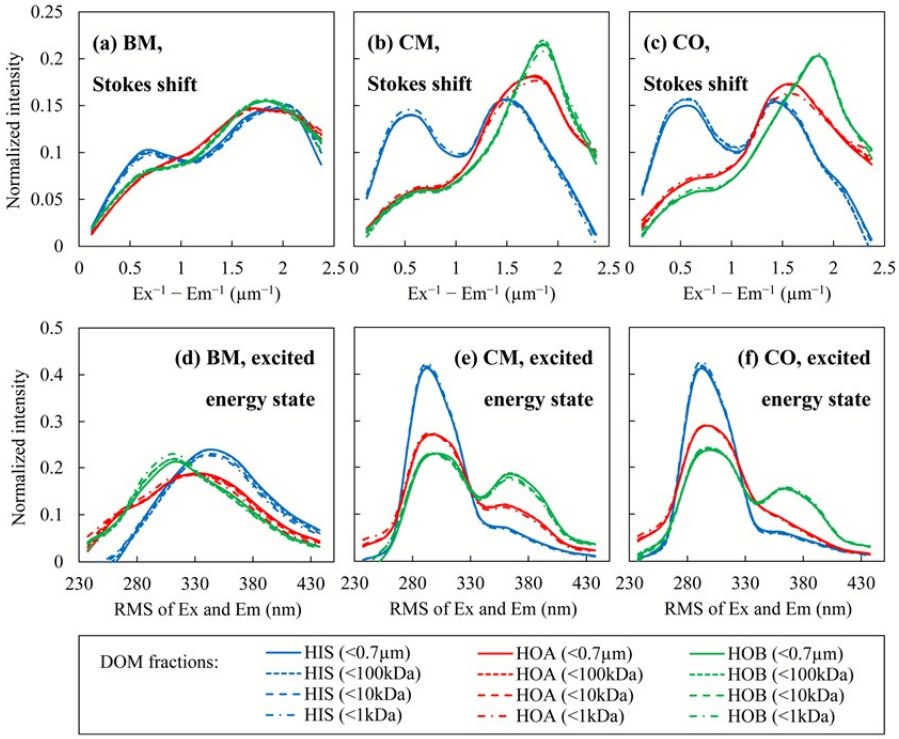

Fig. 5 Distributions of Stokes shift (measured by Ex^{-1}–Em^{-1}, a–c) and excited energy state (measured by RMS of Ex and Em, d–f) based on fluorescence intensity of DOM fractions.

and emission light frequencies, one may also evaluate the mean energy level of the excited state by using, e.g., the reciprocal of RMS of Ex and Em. Scheme 1(b) shows a contour plot of Stokes shift and RMS of Ex and Em in an EEM map. Contours of both formed an approximately perpendicular grid. From the upper left to the lower right of the EEM map, Stokes shift increases gradually; from the lower left to the upper right, RMS of Ex and Em increases (i.e., the mean energy level of the excited state falls).

By mapping the contours onto the actural EEM spectra of the DOM fractions, one can calculate the distributions of Stokes shift (Fig. 5(a–c)) and RMS of Ex and Em (Fig. 5(d–f)) in terms of fluorescence intensity. The Stokes shifts of the hydrophilic fraction HIS were generally smaller than the hydrophobic fractions of HOA and HOB. There were significant intensity peaks for HIS at smaller Stokes shifts (Ex^{-1}–Em^{-1} < 1 μm^{-1}, Fig. 5(a–c)). The hydrophobic fractions had larger Stokes shifts, i.e. greater energy loss in vibrational relaxation, probably because they contained larger π-conjugated systems. Stokes shift of a fluorophore can be expressed by Lippert–Mataga equation:[22]

$$\mathrm{Ex}^{-1} - \mathrm{Em}^{-1} = \frac{2\Delta f}{hc}\Delta\mu^2 a^{-3} + \mathrm{const.} \quad (1)$$

where h is Planck's constant, c the speed of light, Δf the orientation polarizability of the solvent (water), $\Delta\mu$ the difference between the excited- and ground-state dipole moments, and a the size of the fluorophore (which could be regarded as a fluorescent segment of a DOM-macromolecule). $\Delta\mu$ reflects the size of the π-conjugated system, which is proportional to the π-conjugation length.[42] Thus $\Delta\mu^2 a^{-3}$ corresponds to the "coverage rate" of π-conjugation in the fluorophore. It is reasonable that the hydrophobic fractions, with higher aromaticity, should contain segments with larger values of $\Delta\mu^2 a^{-3}$, therefore larger Stokes shifts than the hydrophilic fraction. On the other hand, the Stokes shift distributions barely changed with molecular weight of the DOM fractions (Fig. 5(a–c)).

As for the distributions of RMS of Ex and Em, the peak locations and heights also varied with the hydrophobic/hydrophilic DOM fractions (Fig. 5(d–f)). However, there was no consistency among the three WWTPs as to which fraction had generally the largest or smallest RMS of Ex and Em. On the other hand, the three WWTPs seemed to agree on the weak dependence of RMS upon molecular weight. With the decrease of molecular weight, the fluorescence-intensity-weighed average RMS (calculated from the distribution curves in Fig. 5(d–f)) decreased slightly (the Spearman's rank correlation coefficients ranging from 0.8 to 1, with the exception of CO-HOB), as revealed in Table S2. Speculatively, this trend might be related to the size of fluorophores. It is assumed that in a same pool of organics, smaller molecules are more probable to bear smaller fluorophores. It is generally recognized that smaller fluorophore leads to a greater energy gap between the highest occupied molecular orbital (HOMO) and the lowest unoccupied molecular orbital (LUMO);[22] therefore more energy is required for electronic excitation, corresponding to a higher energy level of the excited state (relative to the ground state), i.e. smaller RMS of Ex and Em.

HPSEC-FLD. The likely dependence of fluorescence on molecular weight was further examined from another perspective using HPSEC-FLD, which gives fluorescent signals across a continuous range of molecular weight from 0.1 to 600 kDa. HPSEC-FLD was particularly competent to explore the fluorescent information of low-molecular-weight substances (<1 kDa) that successive ultrafiltration could not specify. Fig. 6 presents the HPSEC-FLD chromatograms of the different hydrophobic/hydrophilic DOM fractions from the three WWTPs. The fluorescent signals were detected at four excitation/emission-wavelength pairs, i.e. Ex(nm)/Em(nm) = 230/340, 280/340, 310/390, and 250/430, corresponding to the main fluorescence peaks in the typical EEM regions for proteins, microbial byproducts, humic acids, and fulvic acids, respectively (cf. Table S1). Moreover, the four Ex/Ems represent different levels of Stokes shift and excited energy state.

In Fig. 6, longer elution time indicates smaller molecular weight. For smaller molecular weights (e.g. elution time larger than 45 min), stronger fluorescence signals were observed at Ex/Em = 230/340 and 280/340. The two wavelength locations have notebly smaller RMS of Ex and Em (around 300) than those at Ex/Em = 310/390 and 250/430 (RMS around 350), corresponding to higher energy level of the excited state. This was consistent with the finding in the previous section that the smaller DOM molecules tend to be fluorescent at smaller RMS of Ex and Em.

Discussion on the correlation between fluorescent properties and hydrophobicity/ molecular weight

Correlation between fluorescent properties and hydrophobicity. The DOM from the three WWTPs showed consistent trends in that hydrophobic fractions had larger quantum yield and Stokes shift than the hydrophilic. These trends seemed reasonable from a perspective of molecular structure. Auqatic hydrophobic materials normally have higher aromaticity,[1,43] as contributed by aromatic proteins/peptides or polycyclic phenols. Concomitantly, large π-conjugated systems of these molecules often give rise to larger quantum yields and Stokes shifts.[22,42]

Correlation between fluorescent properties and molecular weight. Fluorophore density of the DOM increased remarkably with decreasing molecular weight. Also, a weak positive correlation between the excited-state energy level and molecular weight was traceable, from the results of FRI distribution, RMS of Ex and Em, and HPSEC-FLD. A plausible explanation is that smaller fluorophores undergo greater exposure to light and larger energy gap for excitation.[22] But different molecular-weight subclasses of DOM might intrinsically have different fluorophore structures, which makes the case more blurred.

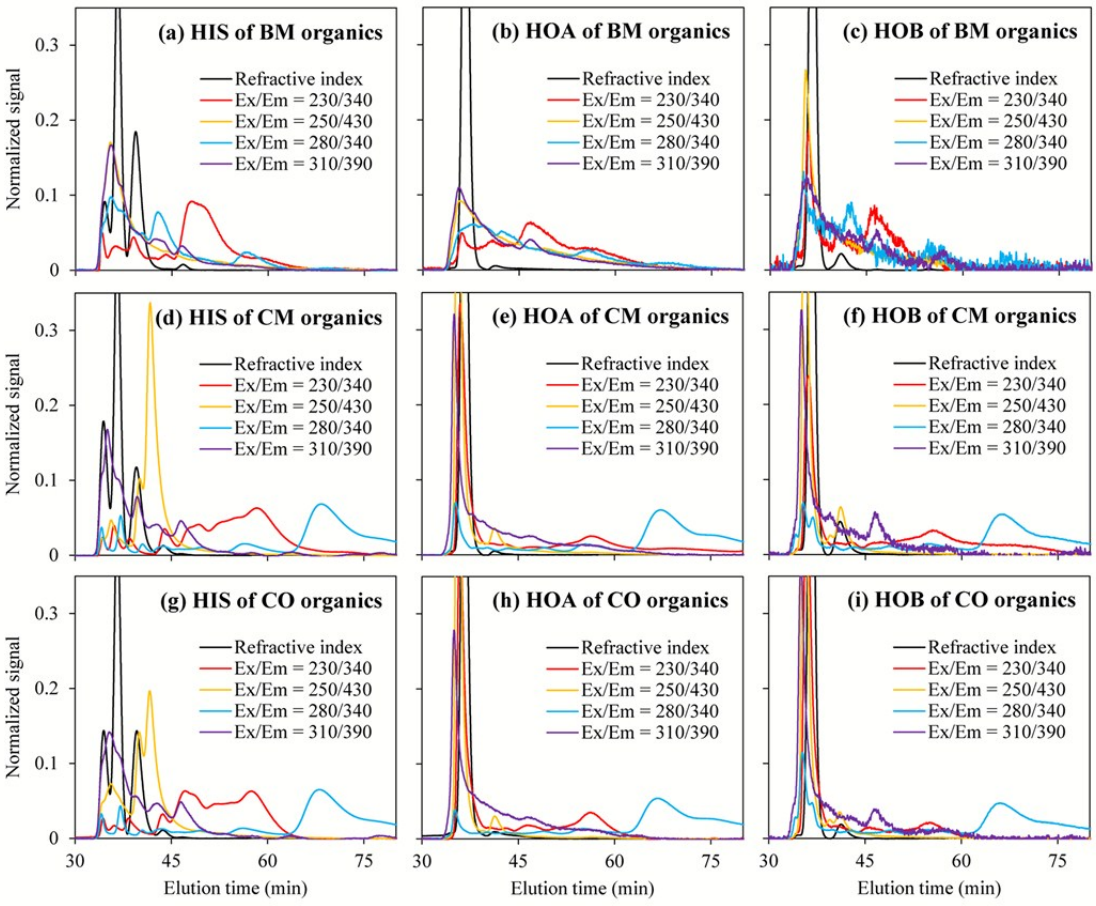

Fig. 6 HPSEC-FLD chromatograms of DOM fractions with different hydrophobicity from the BM, CM, and CO plants.

Other factors affecting fluorescent properties. Fluorescent properties of DOM were also affected by wastewater sources and treatment process configurations.

The wastewater source of the CM and CO plants was a mixture of domestic and industrial wastewaters, while that of the BM plant was purely domestic. This should be responsible for the inter-plant differences in DOM fluorescent properties including: EEM appearance, PARAFAC components, FRI contribution, fluorescence indices, and overall level of fluorophore density. Additionally, the EEM spectra of the influent wastewaters of the three WWTPs are provided in Fig. S6.

Although sharing the same wastewater source, the CM and CO plants had different process configurations (adopting MBR and oxidation ditch respectively), leading to different conditions for pollutant degradation and separation. MBR had longer sludge retention time (20 vs. 12 d), higher sludge concentration (~4 vs. 2 gMLVSS/L), and lower food-to-microorganism ratio (0.16 vs. 0.32 kgBOD_5/(kgVSS·d)), which could facilitate degradation of organics (91%±5% vs. 87%±7% of chemical oxygen demand removal efficiency based on annual average). The undegraded would be partly retained by the membrane (nominal pore size 0.1 μm) and accumulate in the mixed liquor. Thereupon, the accumulation of some less degradable fluorescent material may provide the CM organics with higher fluorophore density than the CO organics. The differences between the CM and CO organics in PARAFAC components, FRI contribution, and fluorescence indices should have also originated from the different process configurations.

Despite the external effect of wastewater source and process configuration, universal trends were found among the three WWTPs in the seemingly internal linkages between DOM fluorescence and hydrophobicity/molecular weight. The DOM fractions exhibited: (a) larger Stokes shift for higher hydrophobicity, (b) larger AFI/UV for higher hydrophobicity, and (c) larger AFI/TOC for smaller molecular weight. These three fluorescence parameters may be potential proxies of DOM hydrophobicity/molecular weight for future application. For example, there is a prospect that in a WWTP with online fluorescence monitoring equipment, given a relatively stable external conditions (such as wastewater source), Stokes shift or AFI/UV may quickly reflect changes in DOM hydrophobicity, which will be conducive to smart operation of the process. One should note that, since DOM is a complex of molecules with various fluorescent characteristics, these linkages may not be accurate in every detail, but rather a macroscopic reflection of collective properties of DOM. In order to make these potential fluorescence proxies practicable, the "universal" trends found in the present three WWTPs will need to be confirmed by extended case studies over a range of WWTPs during long-term operation.

Conclusions

Three WWTPs with different wastewater sources and process configurations (two MBRs and an OD) were investigated to explore the dependence of EEM fluorescent properties on hydrophobicity/molecular weight of DOM. Uniform trends were found in that:

(a) the hydrophobic fractions had higher fluorescence intensity per UV absorbance (indicating higher quantum yield) and larger Stokes shifts than the hydrophilic;

(b) the lower-molecular-weight fractions had higher fluorescence intensity per TOC (indicating higher fluorophore density), with the fluorescence distributed at slightly smaller RMS of Ex and Em.

These trends were explained from the perspective of fluorophore energy state. Smaller RMS of Ex and Em means larger energy gap for electronic excitation, and larger Stokes shift means more energy loss due to vibrational relaxation. Both are critically affected by the scale of π-conjugated system in a fluorophore, and hence possibly linked to hydrophobicity and molecular weight.

Extended investigation would be required to confirm the potential commonness of these trends over a range of wastewater systems.

Acknowledgements

This work was supported by the National Natural Science Foundation of China (No. 21407147), the special fund of State Key Joint Laboratory of Environment Simulation and Pollution Control (No. 14K03ESPCT), and the International Program of MOST (No. 2013DFG92240).

Notes and references

1 J. A. Leenheer and J.-P. Croué, *Environ. Sci. Technol.*, 2003, **37**, 18A-26A.

2 S. K. L. Ishii and T. H. Boyer, *Environ. Sci. Technol.*, 2012, **46**, 2006-2017.

3 R. K. Henderson, A. Baker, K. R. Murphy, A. Hambly, R. M. Stuetz and S. J. Khan, *Water Res.*, 2009, **43**, 863-881.

4 F. Meng, A. Drews, R. Mehrez, V. Iversen, M. Ernst, F. Yang, M. Jekel and M. Kraume, *Environ. Sci. Technol.*, 2009, **43**, 8821-8826.

5 S. Xue, Q. Zhao, L. Wei, X. Hui, X. Ma and Y. Lin, *Front. Environ. Sci. Eng.*, 2012, **6**, 784-796.

6 C. J. van Oss, *Interfacial Forces in Aqueous Media*, Taylor & Francis, Boca Raton, 2nd ed., 2006.

7 K. Xiao, Y.-X. Shen, S. Liang, P. Liang, X.-M. Wang and X. Huang, *J. Membr. Sci.*, 2014, **467**, 206-216.

8 S. Bala Subramanian, S. Yan, R. D. Tyagi and R. Y. Surampalli, *Water Res.*, 2010, **44**, 2253-2266.

9 M. Wloka, H. Rehage, H. C. Flemming and J. Wingender, *Colloid Polym. Sci.*, 2004, **282**, 1067-1076.

10 Z. Wang, C. M. Hessler, Z. Xue and Y. Seo, *Water Res.*, 2012, **46**, 1052-1060.

11 K. Xiao, X. Wang, X. Huang, T. D. Waite and X. Wen, *J. Membr. Sci.*, 2011, **373**, 140-151.

12 Y. X. Shen, W. T. Zhao, K. Xiao and X. Huang, *J. Membr. Sci.*, 2010, **346**, 187-193.

13 G. R. Aiken, D. M. McKnight, K. A. Thorn and E. M. Thurman, *Org. Geochem.*, 1992, **18**, 567-573.
14 N. Her, G. Amy, D. McKnight, J. Sohn and Y. M. Yoon, *Water Res.*, 2003, **37**, 4295-4303.
15 C. F. Galinha, G. Carvalho, C. A. M. Portugal, G. Guglielmi, R. Oliveira, J. G. Crespo and M. A. M. Reis, *Water Sci. Technol.*, 2011, **63**, 1381-1388.
16 N. Hudson, A. Baker and D. Reynolds, *River Res. Applic.*, 2007, **23**, 631-649.
17 Z. Wang, Z. Wu and S. Tang, *Water Res.*, 2009, **43**, 1533-1540.
18 J. R. Lakowicz, *Principles of Fluorescence Spectroscopy*, Springer, New York, 3rd ed., 2006.
19 P. G. Coble, J. Lead, A. Baker, D. M. Reynolds and R. G. M. Spencer, *Aquatic Organic Matter Fluorescence*, Cambridge University Press, New York, 2014.
20 H. Yu, Y. Song, R. Liu, H. Pan, L. Xiang and F. Qian, *Chemosphere*, 2014, **113**, 79-86.
21 W. Chen, P. Westerhoff, J. A. Leenheer and K. Booksh, *Environ. Sci. Technol.*, 2003, **37**, 5701-5710.
22 B. Valeur and M. N. Berberan-Santos, *Molecular Fluorescence: Principles and Applications*, Wiley-VCH, Weinheim, Germany, 2nd ed., 2012.
23 H.-C. Kim and B. A. Dempsey, *Water Res.*, 2012, **46**, 3714-3722.
24 C. A. Stedmon and R. Bro, *Limnol. Oceanogr. Methods*, 2008, **6**, 572-579.
25 A. Huguet, L. Vacher, S. Relexans, S. Saubusse, J. M. Froidefond and E. Parlanti, *Org. Geochem.*, 2009, **40**, 706-719.
26 C. A. Parker and W. T. Rees, *Analyst*, 1960, **85**, 587-600.
27 A. T. R. Williams, S. A. Winfield and J. N. Miller, *Analyst*, 1983, **108**, 1067-1071.
28 Y.-X. Shen, K. Xiao, P. Liang, J.-Y. Sun, S.-J. Sai and X. Huang, *J. Membr. Sci.*, 2012, **415-416**, 336-345.
29 M. Dubois, K. A. Gilles, J. K. Hamilton, P. A. Rebers and F. Smith, *Anal. Chem.*, 1956, **28**, 350-356.
30 Y.-X. Shen, K. Xiao, P. Liang, Y.-W. Ma and X. Huang, *Appl. Microbiol. Biotechnol.*, 2013, **97**, 4167-4178.
31 M. Hof, V. Fidler and R. Hutterer, in: M. Hof, R. Hutterer and V. Fidler (Eds.), *Fluorescence Spectroscopy in Biology: Advanced Methods and Their Applications to Membranes, Proteins, DNA, and Cells*, Springer-Verlag Berlin Heidelberg, Berlin; Heidelberg, 2005, pp. 3-29.
32 M. Bahram, R. Bro, C. Stedmon and A. Afkhami, *J. Chemometr.*, 2006, **20**, 99-105.
33 T. Ohno, *Environ. Sci. Technol.*, 2002, **36**, 742-746.
34 A. J. Lawaetz and C. A. Stedmon, *Appl. Spectrosc.*, 2009, **63**, 936-940.
35 R. Lapasin and S. Pricl, *Rheology of Industrial Polysaccharides: Theory and Applications*, Blackie Academic & Professional, London; New York, 1st ed., 1995.
36 O. H. Lowry, N. J. Rosebrough, A. L. Farr and R. J. Randall, *J. Biol. Chem.*, 1951, **193**, 265-275.
37 V. L. Singleton, R. Orthofer and R. M. Lamuela-Raventós, in: P. Lester (Eds.), *Methods in Enzymology*, Academic Press, 1999, pp. 152-178.
38 J. Wu and X. Huang, *J. Membr. Sci.*, 2009, **342**, 88-96.
39 W.-T. Zhao, Y.-X. Shen, K. Xiao and X. Huang, *Bioresource Technol.*, 2010, **101**, 3876-3883.
40 J. Chen, E. J. LeBoeuf, S. Dai and B. Gu, *Chemosphere*, 2003, **50**, 639-647.
41 W. Liao, R. F. Christman, J. D. Johnson, D. S. Millington and J. R. Hass, *Environ. Sci. Technol.*, 1982, **16**, 403-410.
42 Y. Yamaguchi, Y. Matsubara, T. Ochi, T. Wakamiya and Z.-i. Yoshida, *J. Am. Chem. Soc.*, 2008, **130**, 13867-13869.
43 L. H. Fan, J. L. Harris, F. A. Roddick and N. A. Booker, *Water Res.*, 2001, **35**, 4455-4463.

Graphical abstract